JOURNAL OF SPACECRAFT AND ROCKETS
Vol. 32, No. 2, March–April 1995

Microstructural Damage and Fracture Processes in a Composite Solid Rocket Propellant

C. D. Bencher *
University of California and Lawrence Berkeley Laboratory, Berkeley, California 94720-1260
R. H. Dauskardt†
Stanford University, Stanford, California 94305
and
R. O. Ritchie‡
University of California and Lawrence Berkeley Laboratory, Berkeley, California 94720-1260

A study has been made of the microstructural damage and fracture processes associated with the fracture-toughness behavior of a polymer-matrix composite solid rocket-propellant material. Specifically, nonlinear-elastic fracture-mechanics tests were performed, as a function of displacement rate and temperature (−54 to 71°C), on center-cracked sheet test samples to determine fracture toughness in the form of J-integral resistance curves and viscoelastic resistance curves for the inert propellant H-24; in addition, in situ video imaging was employed to characterize the deformation and interaction between microstructural features and the crack-path morphology. It was found that at the lowest temperatures the increased polymer matrix strength resulted in enhanced cavitation and particle delamination, leading to larger crack-tip fracture process zones and hence to higher fracture toughness. At the high temperatures, the weaker polymer matrix was seen to tear readily and to advance the crack before significant particle delamination or cavitation would occur; this mechanism resulted in small fracture process zones and accounts for the decrease in fracture toughness with increasing temperature. The relationships between the toughness and fracture process in the material are discussed in terms of characterizing parameters for microstructural damage.

Nomenclature

a = crack length, mm
B = specimen thickness, mm
b = uncracked ligament, mm
C^* = rate-dependent analog of J, $\mathrm{kJ \cdot m^{-2} \cdot s^{-1}}$
d_n = constant relating crack-tip opening displacement and J (dependent upon n and σ_0/E)
E = Young's modulus, MPa
E' = $E/(1-\nu^2)$ in plane strain, E in plane stress, MPa
E_R = reference modulus, defined as the short-time ($t = 0$) relaxation modulus, MPa
$E(t)$ = time-dependent Young's modulus, MPa
$\bar{E}(t)$ = time-averaged Young's modulus, MPa
$F(a/b)$ = function, dependent upon a/b, relating K_I to σ
h_1, h_3 = functions of n and a/W in Eq. (3)
J = J integral, $\mathrm{kJ \cdot m^{-2}}$
J_C = critical value of J at crack initiation, $\mathrm{kJ \cdot m^{-2}}$
J_{IC} = plane-strain fracture toughness, defined in terms of J, $\mathrm{kJ \cdot m^{-2}}$
J_R = crack-growth resistance, defined in terms of J, $\mathrm{kJ \cdot m^{-2}}$
$J_R(\Delta a)$ = resistance curve, defined in terms of J_R and crack extension Δa
J_V = viscoelastic J integral, $\mathrm{kJ \cdot m^{-2}}$
$J_V(\Delta a)$ = resistance curve, defined in terms of J_V and crack extension Δa
K = stress-intensity factor, $\mathrm{MPa \cdot m^{\frac{1}{2}}}$
K_C = critical value of K at crack initiation (instability), $\mathrm{MPa \cdot m^{\frac{1}{2}}}$
K_I = mode I stress-intensity factor, $\mathrm{MPa \cdot m^{\frac{1}{2}}}$
K_{IC} = plane-strain fracture toughness, defined in terms of K_I, $\mathrm{MPa \cdot m^{\frac{1}{2}}}$
$K_\mathrm{I}(\Delta a)$ = resistance curve, defined in terms of K_I as a function of Δa
k = exponent in the crack-velocity–J_V relationship
n = strain-hardening exponent relating stress and plastic strain
n' = strain-hardening exponent, relating stress and pseudoelastic strain
P = applied load, N
p = exponent in Eq. (8), equal to $[(1+n')/n']k$
S_p = Schapery's damage parameter
t = time, s
v = crack velocity, $\mathrm{mm \cdot s^{-1}}$
W = specimen width, mm
$\bar{z}$ = integration variable in Eq. (6)
α = constant, or order unity, in constitutive law
Δ = displacement, mm
Δ^e = pseudoelastic displacement, mm
Δa = crack extension, mm
$\Delta\delta$ = load-line displacement, mm
δ_t = crack-tip opening displacement, mm
ε = strain
ε^e = pseudoelastic displacement
ε_0 = reference strain, defined as the flow strain
$\varepsilon_{\mathrm{pl}}$ = plastic strain
η = geometry-dependent factor, which is a function of a and n
ν = Poisson's ratio
σ = stress, MPa
σ_0 = flow stress, MPa
σ_{TS} = (ultimate) tensile stress, MPa

Received Feb. 16, 1994; revision received July 21, 1994; accepted for publication Aug. 2, 1994. This paper is declared a work of the U.S. Government and is not subject to copyright protection in the United States.

*Graduate Student, Department of Materials Science and Mineral Engineering, University of California, and Center for Advanced Materials, Materials Sciences Division, Mail Stop 66-200.

†Assistant Professor, Department of Materials Science and Engineering.

‡Professor, Department of Materials Science and Mineral Engineering, University of California, and Center for Advanced Materials, Materials Sciences Division, Mail Stop 66-200.

Introduction

THE use of solid rocket propellants for the propulsion of space launch vehicles is well known. In the design of such ballistic engines, it is first necessary to determine the mechanical properties of the solid composite propellant to be used so as not to impose damaging loads upon the fuel.[1] However, damage in such propellants due to incipient cracking or microvoid formation[2] has recently become of some concern, as it can lead to structural problems and can alter the burn rate of the propellant. To address this issue, the current study was instigated to examine the development of microstructural damage and fracture processes in a polymer-matrix composite solid rocket-propellant material as a function of strain rate and temperature, and to relate such processes to the fracture toughness of the material.

As the deformation behavior of polymeric solid rocket propellants is highly nonlinear,[3,4] the toughness properties of the H-24 material were evaluated using nonlinear-elastic fracture-mechanics methods. Although the stress intensity K_I and the conventional J integral were originally derived for rate-independent behavior, a number of investigators have reported linear-elastic and elastic-plastic fracture toughness values K_{IC} and J_{IC}, stress-intensity crack-resistance curves $K_I(\Delta a)$, and energy-release-rate crack-resistance curves $J_R(\Delta a)$ for plastics, utilizing testing and data analysis techniques virtually identical to those used in the study of quasistatic behavior in metals.[5-8] The validity of K and J is not guaranteed, however, when a material exhibits rate-dependent mechanical properties.

The conventional J integral will uniquely characterize the crack-tip conditions in a viscoelastic material only for a given failure time; a critical J value taken from a laboratory test is relevant to a structure only if different samples have similar failure times. A constant-rate J test can provide a rational measure of fracture toughness in polymers, but applying such data to structural components is difficult. To take account of the time dependence of viscoelastic materials, Schapery[9,10] has proposed a characterizing parameter, J_V, which is analogous to C^* (the viscous analog of J) used in describing such time-dependent behavior as creep crack growth in metals. For a material that obeys the assumed constitutive law, Schapery showed that J_V uniquely defines the crack-tip conditions, making it a suitable fracture criterion for a wide range of rate-sensitive materials. In the present study, the fracture toughness of H-24 was therefore measured at selected temperatures using both conventional J-integral techniques and Schapery's viscoelastic, time-dependent approach. The validity of the two approaches in properly characterizing the crack-tip strain fields is evaluated by comparing measured crack opening displacements with values predicted from the J_R and J_V measurenents.

Experimental Procedures

Materials

The polymer-composite solid rocket propellant chosen for study, H-24, consists of a hydroxyl-terminated polybutadiene rubber matrix containing ≈200-μm-size potassium chloride particles and a bimodal distribution of metallic aluminum particles in ≈5- and ≈20-μm sizes; the potassium chloride and aluminum particles make up ≈70% and ≈20% of the propellant by weight, respectively. Although H-24 is an inert propellant that contains potassium chloride in place of ammonium chloride, the material is thought to mimic qualitatively the deformation and fracture characteristics of active propellant.

Fracture Toughness Testing

The fracture toughness of H-24 was measured as a function of temperature and displacement rate, using both the J-resistance curve $J_R(\Delta a)$ and the viscoelastic, time-dependent J_V, on center-cracked sheet tensile specimens [middle-tension, M(T) panels], where crack lengths and damage processes were monitored in situ using a video imaging and recording system. Crack length was measured to a resolution of ±0.25 mm. Test specimens 110 mm long, 50 mm wide, and 5 mm thick, with ≈5 mm-long precracks (produced by surgical scalpel cuts)[11] emanating from a 3-mm-diam center hole, were deformed in tension on a servohydraulic testing machine at three different displacement rates. These rates, which were typical of field operation, were 8.4, 6.4, and 3.2 mm · min^{-1}, corresponding approximately to initial far-field strain rates of 0.09, 0.07, and 0.03 min^{-1}. Tests were performed at three different temperatures, specifically −54, 25, and 71°C, chosen to represent the minimum, maximum, and room temperatures experienced during storage, transport, and use of the launch vehicles. Temperatures were maintained to within ±5°C using a thermocouple and feedback controller involving heat lamps and liquid-nitrogen cooling.

In order to compute J-integral[12] values, the constitutive properties of H-24 were first determined on unnotched tensile sheet specimens tested at identical temperatures and displacement rates; data were fit to the power-law hardening expression relating stress to plastic strain:

$$\frac{\varepsilon_{pl}}{\varepsilon_0} = \alpha \cdot \left(\frac{\sigma}{\sigma_0}\right)^n \tag{1}$$

where n is the strain-hardening exponent. The value of J was calculated from the stress intensity in terms of its elastic and plastic components from measurements of the applied load and load-line displacement, using[13]

$$J = \underbrace{\frac{K_I^2}{E'}}_{\text{elastic}} + \underbrace{\frac{\eta}{Bb}\int_0^{\Delta\delta} P \cdot \mathrm{d}\Delta\delta}_{\text{plastic}} \tag{2}$$

where the geometry-dependent factor η is a function of the crack size and the strain-hardening coefficient. The integral in Eq. (2) was evaluated, using standard numerical integration methods, from test data on load vs load-line displacement. For the center-cracked sheet sample,[13]

$$\eta = \frac{n+1}{n} \cdot \frac{h_1}{2Wh_3} \tag{3}$$

where W is the specimen half width, and h_1 and h_3 are both functions of n and the crack length-to-width ratio, a/W. Stress intensities were determined from handbook solutions[14] in terms of the applied stress and half crack length, using

$$K_I = \sigma\sqrt{\pi a} \cdot F(a/b) \tag{4}$$

where

$$F(a/b) = 1 + 0.128(a/b) - 0.288(a/b)^2 + 1.525(a/b)^3$$

The viscoelastic integral J_V was computed by removing the creep displacements arising from the material's viscous behavior that occur during the time of the fracture test and adjusting the curve of load vs load-line displacement (P-Δ curve) into a curve of load vs *pseudoelastic displacement* (P-Δ^e curve). This was achieved by performing a stress relaxation test at each of the relevant temperatures, and dividing the measured stress as a function of time, $\sigma(t)$, by the constant strain, in order to calculate the effective Young's modulus as a function of time, $E(t)$.[9,10] For a constant-displacement-rate fracture test, the pseudoelastic displacement is then given by

$$\Delta^e = \Delta \cdot \frac{\bar{E}(t)}{E(R)} \tag{5}$$

To reflect accurately the physics of the relaxation in displacement due to creep, the reference modulus E_R is defined specifically as the short-time relaxation modulus, taken at time $t = 0$. The time-averaged modulus $\bar{E}(t)$ is given in terms of an integration variable $\bar{z}$ by[9,10]

$$\bar{E}(t) = \frac{1}{t}\int_0^t E(t-\bar{z})\,\mathrm{d}t \tag{6}$$

The time-averaged modulus $\bar{E}(t)$ is independent of the strain applied in the stress relaxation test if the polymer is linear-viscoelastic.

A polymer is linear-viscoelastic if after removing the relaxation strains, the curve of load vs pseudoelastic displacement (P-Δ^e curve) is linear, which is not the case for the solid rocket propellant. However, at small strains ($\varepsilon \leq 3\%$), the experimentally determined relaxation modulus is not very sensitive to the strain level, and can be used to evaluate pseudoelastic strains.[15] Viscoelastic resistance curves $J_V(\Delta a)$ were determined by integrating the P-Δ^e curves.

Results and Discussion

Fracture-Toughness Measurements

The stress-strain curves used to calculate material constitutive properties are shown in Fig. 1 for three strain rates at 25°C, and for one strain rate at −54 and 71°C. It is apparent that the strength of the polymer increases rapidly at lower temperatures (strengths are 4 to 5 times higher at −54°C than at 25°C), with strain-hardening exponents varying between 3 and 7; the properties are listed in Table 1. Figure 2 presents the stress relaxation data used to convert the actual displacements into pseudoelastic displacements for the curves of load vs load-line displacement seen in Fig. 3. These curves reflect the reduction in integrated area (energy) calculated after removing the creep strains from the viscoelastic behavior. These reduced energies account for the decreased viscoelastic J_V values in comparison with the conventional J values in the crack-length resistance curves presented in Fig. 4. The separate elastic and inelastic contributions to the conventional J integral, shown in Fig. 5, illustrate the dominance of the inelastic energy absorbed in the fracture process, indicating that the majority of the energy absorbed during fracture takes place in the process zone ahead of the crack tip; toughness is therefore markedly controlled by the size and behavior of the process zone.

These results show the trend of increasing fracture toughness with decrease in temperature (Fig. 4), which is in part related to the increased tensile strength of the polymer at lower temperatures (Fig. 1). (This trend is not shown by the 71°C fracture toughness results, because of limitations in the calculations that are discussed

Table 1 Material properties for H-24 propellant

Temperature, °C	−54	25	71
Tensile strength σ_{TS}, MPa	2.04	0.42	0.15
Reference modulus[a] E_R, MPa	56.5	24.8	9.4
Strain-hardening coeff.[b] n	4.42	6.93	3.67
Yield strength[c] σ_0, MPa	0.736	0.251	0.026

[a]Defined as the Young's modulus at time $t = 0$.
[b]Defined at a displacement rate of 6.37 mm/min.
[c]Defined as 0.02% offset stress.

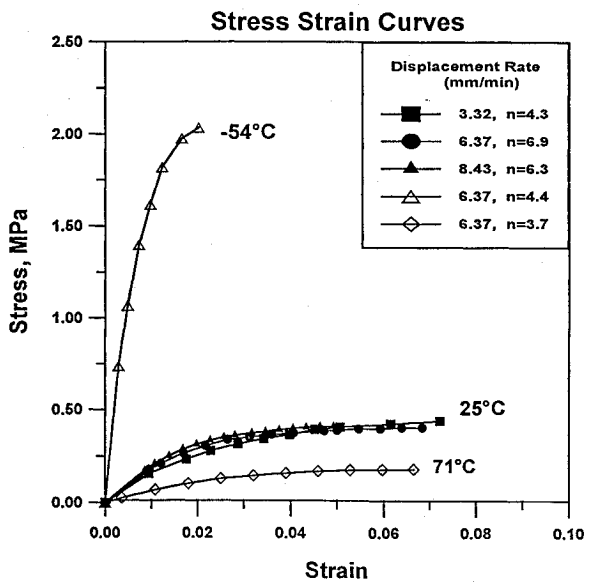

Fig. 1 Plot of stress-strain constituitive behavior at varying temperatures and strain rates.

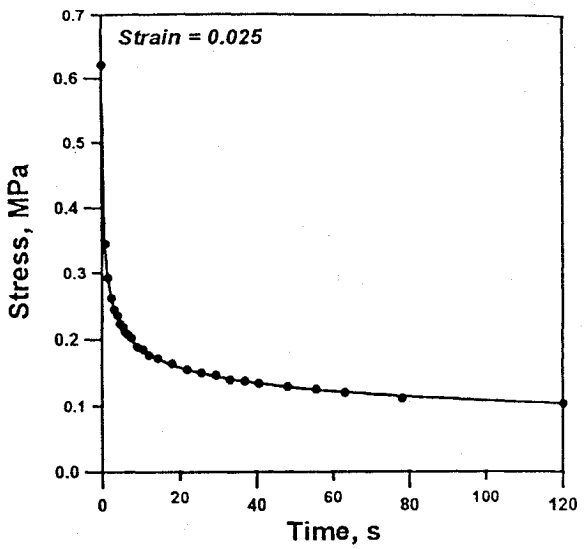

a) 25°C

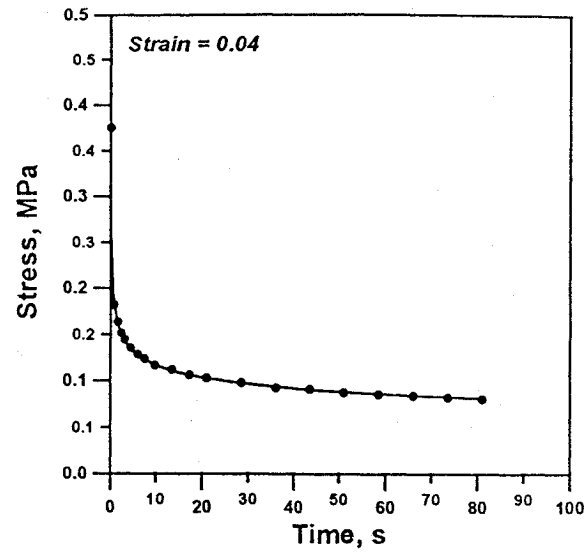

b) 71°C

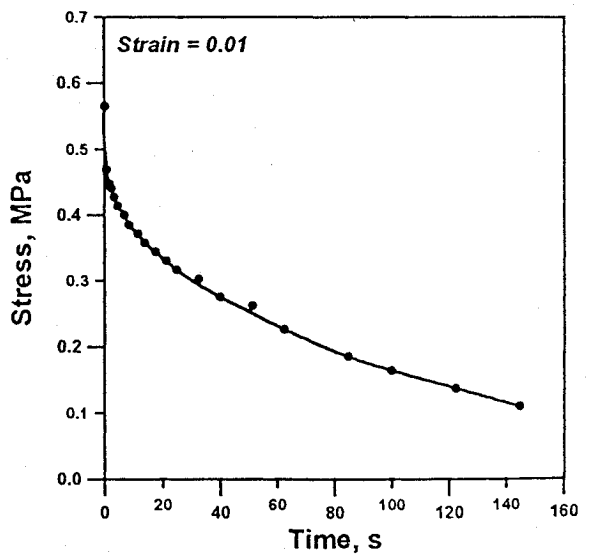

c) −54°C

Fig. 2 Results of stress relaxation tests at various temperatures.

Table 2 Fracture-toughness quantities for H-24 propellant

Temperature, °C	−54	25	71
K_c,[a] MPa · $m^{\frac{1}{2}}$	0.48	0.13	0.08
J_c,[b] kJ/m^2	5.0	2.7	2.5
J_v,[b] kJ/m^2	4.0	0.7	0.6
Measured CTOD, mm	2.0	1.5	0.5
Computed CTOD,[c] mm	2.1	1.2	5.0

[a]From $K_c = \sqrt{J_v E_R}$.
[b]For 6.37-mm/min displacement rate.
[c]From Eq. (7); see Ref. 19.

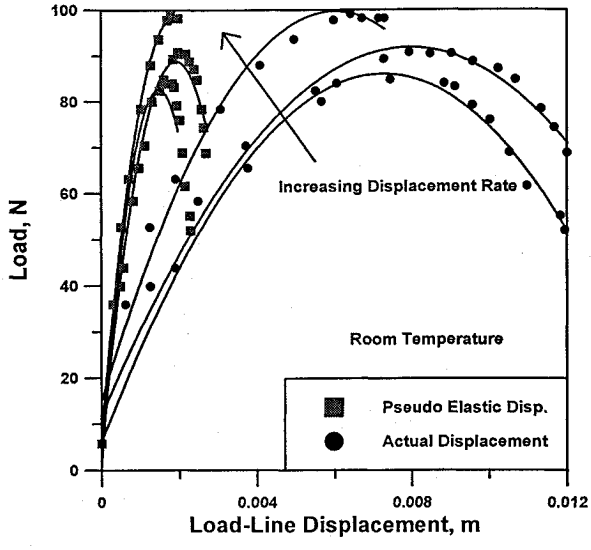

Fig. 3 Plot of load vs actual and pseudoelastic load-line displacements.

below.) At high temperatures above the glass-transition temperature, polymers typically soften and display lower toughness; for example, bridging ligaments within a craze zone rupture at lower stresses before large-scale plastic deformation can occur.

While polymeric materials are generally sensitive to strain rate, no definitive trend was observed in the measured toughnesses (Fig. 4). Overall, the displacement rates were not of sufficient variance to demonstrate a conclusive effect.

These toughness results, listed in Table 2, must be evaluated in terms of the relevance of the integrals J and J_V in characterizing the crack-tip fields in this material. Clearly the conventional J integral does not account for the time-dependent behavior in H-24, and must therefore be considered inappropriate. The J_V integral,[9,10] on the other hand, does allow for a viscoelastic contribution to deformation and in this respect does provide a more appropriate characterizing parameter; however, the validity of J_V in this case will depend critically on the size and geometry of the test specimens.

For the center-cracked sheet M(T) specimen, the dominance of the HRR singularity[16,17] and hence of J in describing the crack-tip stress and deformation fields is assured when the uncracked ligament b exceeds approximately $200J/\sigma_0$ for a material where the strain-hardening exponent $n \approx 5$.[18] For the H-24 material, this requires significantly larger samples (by nearly an order of magnitude for −54°C and 25°C tests, and even more for 71°C tests) for valid toughness measurements. However, crack-tip opening displacements (CTODs) δ_t could be computed from the J_V values using the δ_t-J relationship derived from the HRR singularity fields according to[19]

$$\delta_t = d_n \frac{J}{\sigma_0} \tag{7}$$

where d_n varies from 0.3 to 1, depending upon the strain-hardening coefficient n, the yield strain σ_0/E, and whether plane stress or plane strain conditions are assumed. Such values were found to

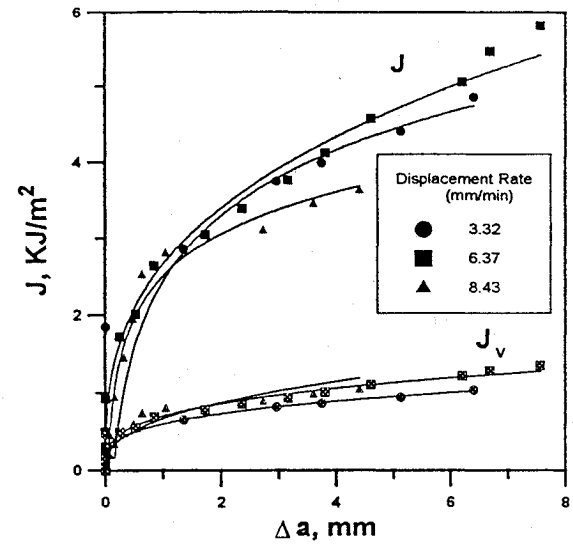

a) 25°C

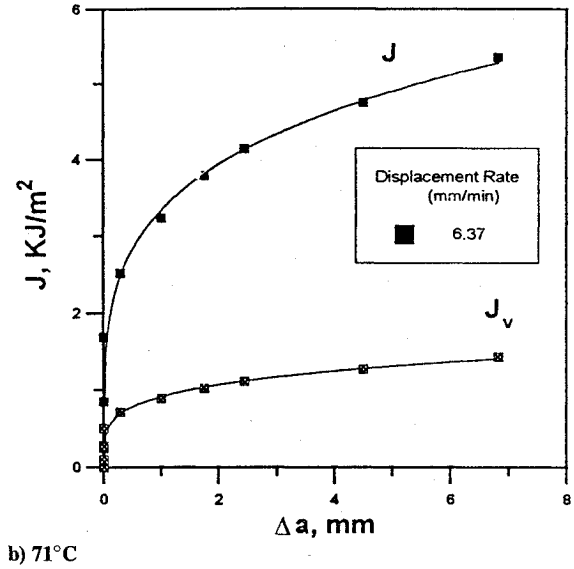

b) 71°C

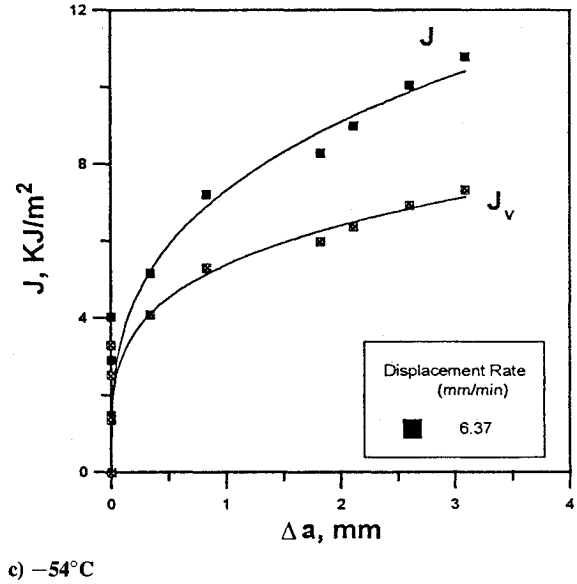

c) −54°C

Fig. 4 Plot of conventional J and viscoelastic J_V integrals vs crack extension for various temperature conditions.

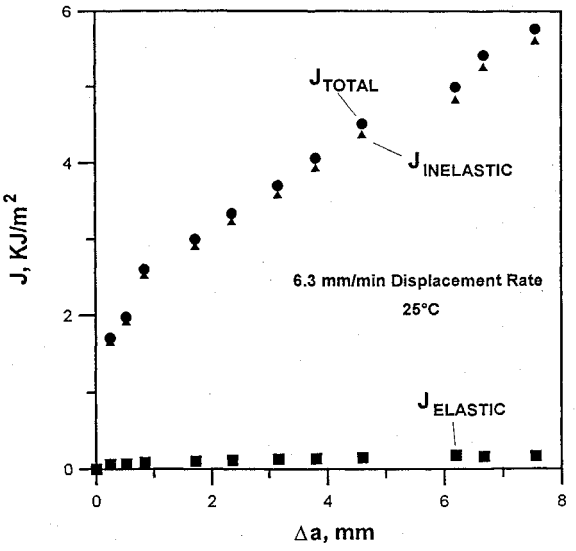

Fig. 5 Plot of elastic and inelastic components of J-integral calculated values.

approximate closely the experimentally measured CTODs determined at −54 and 25°C (Table 2), suggesting that the measured J_V toughness for H-24 over this temperature range is reasonable; J_V values quoted for 71°C, however, are clearly invalid.

Microstructural Damage Mechanisms

Fracture in H-24 was observed to be associated with a crazing mechanism, involving highly localized deformation leading to the growth of microvoids.[20,21] Crack advancement occurs as fibrils at the trailing end of the crazing zone rupture and the voids coalesce with the crack tip. Whereas in a pure polymer the cavitation usually initiates from inorganic dust particles entrapped in the polymer,[22] in H-24 propellant it initiated from the large (≈200 μm) potassium chloride particles, roughly 1 to 2 CTODs ahead of the crack tip, by the mechanism of the polymer matrix debonding from the particle surface (Fig. 6); these voids grow in size as they move closer to the crack tip. This process greatly facilitates the development of the craze, which is further promoted by an enhanced hydrostatic stress state directly ahead of the crack tip.[7] (The location at 1 to 2 CTODs ahead of the crack tip is where triaxiality is maximized for a Prandtl field in plane strain.) The extent of the process zone, within which particle pullout, void growth, and crazing behavior take place, is directly related to the material's fracture toughness.

At room temperature, the process zones were generally on the order of 3.0–3.5 mm in size, defined by the location of initial particle debonding, with measured CTODs of ≈1.5 mm. A sequence showing the progression from initial particle debonding to craze ligament formation and failure is seen in Fig. 7. Microstructural damage was essentially unchanged by varying the displacement rate; all three displacement rates resulted in similar damage and similar damage zone sizes. These near-identical inelastic zone processes and zone sizes are consistent with the insensitivity of the fracture toughness over the range of tested strain rates at this temperature (Fig. 4).

At lower temperatures, −54°C, initial particle debonding and growth again commenced at roughly 1 to 2 CTODs in front of the crack, although the roughly fourfold increase in strength of the polymer matrix resulted in larger rupture strains, as the tensile strength of the ligaments between the voids was considerably greater. This leads to larger process zones, which can exceed 4-mm diam, and correspondingly larger CTODs (≈2.0 mm) (Fig. 8a). The enhanced damage, in the form of a greater percentage of particle pullout, particle debonding further ahead of the crack tip, and larger and more numerous voids, is responsible for the high toughness measured at −54°C. Variations in the strain rate did not appear to cause distinct changes in the extent of microstructural damage.

At elevated temperatures, 71°C, the polymer matrix softened to the point where it would support only small stresses before the craze

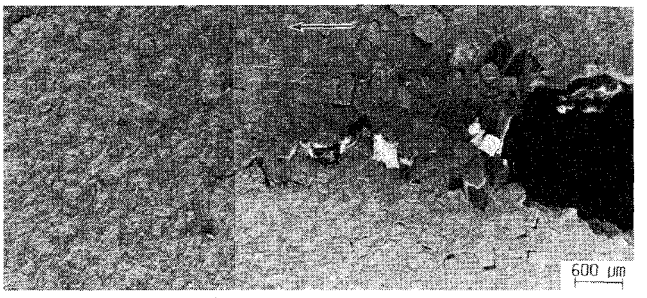

a) Process zone ahead of crack tip

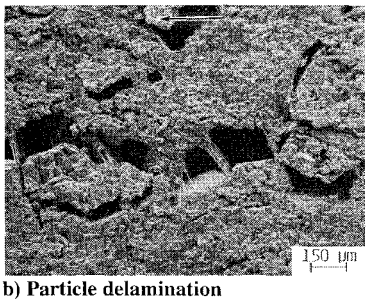

b) Particle delamination

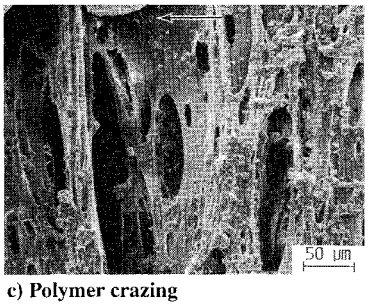

c) Polymer crazing

Fig. 6 Scanning electron micrographs illustrating stages in the fracture process. Arrow indicates the direction of crack growth.

ligaments ruptured. Additionally, the thermal energy facilitates interchain sliding, allowing the ligaments to thin more rapidly and rupture under the lower tensile stress. This leads to smaller process zones ahead of the crack tip (Fig. 8b); the CTODs and process-zone sizes were generally on the order of 0.5 and 1.0 mm, respectively. The behavior once again was essentially unchanged over the range of strain rate studies. Microstructurally, particle delamination, void nucleation, and void growth occurred on a much smaller scale at 71°C; accordingly, the weaker ligament tensile strength and the smaller inelastic process zones yielded the lowest fracture-toughness values.

Damage-Characterizing Parameter

An alternative approach to characterizing microstructural damage and hence toughness can be achieved through the use of damage parameters. One such approach applicable to polymeric composites has been proposed in Ref. 15. Schapery's damage parameter S_p is a calculated prediction of the microstructural damage such as microcracking, void growth, and crazing, and for a given strain, increases in S_p indicate increasing levels of damage. The parameter S_p is measured in a uniaxial tensile test, although its calculation is complicated by the requirement of a constant taken from a crack-velocity–J_V (viscoelastic resistance) relation; this prerequisite of a J-integral fracture-toughness test somewhat limits the usefulness of S_p, as it cannot be deduced solely from uniaxial tensile data. In this approach, damage is defined as[15]

$$S_p = \left(\int_0^t (\varepsilon^e)^p \, dt \right)^{1/p} \tag{8}$$

where the integration over time is performed on uniaxial tensile data, and ε^e is the pseudoelastic strain calculated from pseudoelastic

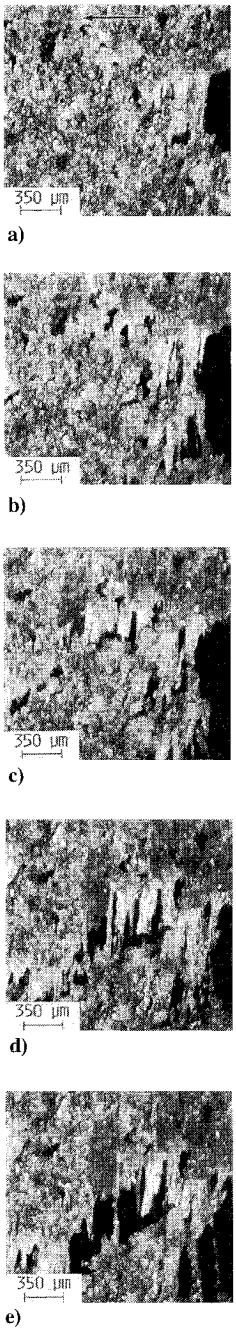

Fig. 7 In situ video images of a sequential progression from initial particle debonding to craze ligament formation and failure at room temperature. Arrow indicates the direction of crack growth.

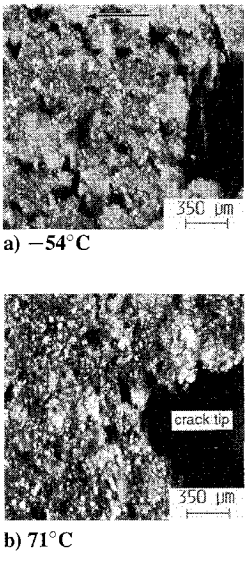

Fig. 8 In situ video images of microstructural damage in the process zone ahead of the crack tip. Arrow indicates the direction of crack propagation.

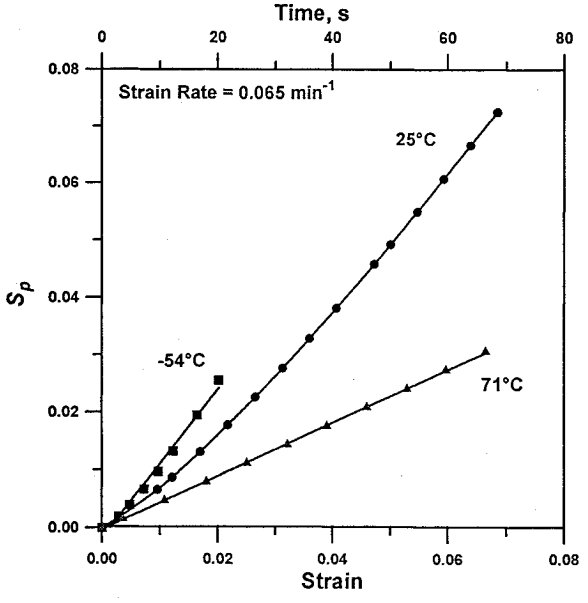

Fig. 9 Schapery's microstructural damage parameter as a function of true strain, plotted at various temperatures.

displacements rather than actual displacements. The constant p is calculated from two other constants:

$$p = \left(\frac{1+n'}{n'}\right)k$$

where n' is taken from the constitutive law relating stress to pseudoelastic strains, $\varepsilon^0 \propto (\sigma)^{n'}$, and k is taken from the crack-velocity–J_V relationship, $v \propto (J_V)^k$.

The computed variation in the damage parameter S_p is shown as a function of true strain for the three temperatures tested in Fig. 9. Inasmuch as this parameter is a calculated prediction of the microstructural damage, it should both be consistent with microstructural observations during fracture, and reveal a similar trend to measured toughness values that are governed by such behavior. The damage-parameter plot of Fig. 9 indicates that microstructural damage should accumulate more rapidly at lower temperatures (at similar strains and strain rates), consistent with observations of increased crack-tip damage and enhanced process zones at −54°C. Accordingly, the measured fracture-toughness behavior (Fig. 4), which is enhanced by increased microstructural damage, is reflected in the damage-parameter predictions. The damage parameter S_p therefore can be utilized as an alternative characterizing parameter providing information regarding microstructural damage and fracture toughness. As stated previously, however, the utility in this approach is somewhat diffused by the prerequisite of a fracture-toughness test.

Conclusions

Based on a study of microstructural damage and fracture-toughness behavior in H-24 solid rocket propellant, at temperatures and strain rates of commercial relevance, the following conclusions can be made. Crack propagation occurs via a crazing fracture mechanism with initial cavitation occurring by polymer matrix delamination around the potassium chloride particles at approximately 1 to 2 CTODs ahead of the crack tip. The highly temperature-dependent properties of the polymer matrix resulted in markedly different levels of microstructural damage over the temperature range −54 to 71°C. Although the behavior was relatively insensitive to

the strain rates tested, with decreasing temperatures the four- to fivefold increase in strength of the polymer matrix led to higher rupture strains in the craze ligaments and to enhanced toughness. Qualitatively, such microstructural damage in fracture tests could be characterized by Schapery's damage parameter, derived primarily from uniaxial tensile data; moreover, the extent of this damage correlated well with fracture-toughness measurements. In this regard, the viscoelastic integral J_V appears to provide an appropriate measure of the toughness of propellant H-24, although specimen size requirements for the validity of J in the center-cracked sheet specimens results in some uncertainty in the J_V values at the higher temperatures.

Acknowledgments

This work was supported by the Astronautics Laboratory of Edwards Air Force Base, CA 93523, under the auspices of the U.S. Department of the Air Force, through the Director, Office of Energy Research, Office of Basic Energy Sciences, Materials Sciences Division of the U.S. Department of Energy under Contract DE-AC03-76SF00098. Thanks are due to C. T. (Jimmy) Liu for providing the propellant material and for many helpful discussions.

References

[1]Bills, K. W., and Wiegard, J. W., "Relation of Mechanical Properties to Solid Rocket Motor Failure," *AIAA Journal*, Vol. 1, No. 9, 1963, pp. 2116–2123.

[2]Knollman, G. C., and Martinson, R. H., "Nonlinear Elastic Effects in the Ultrasonic Assessment of Cumulative Damage in Filled Polymers," *Journal of Applied Physics*, Vol. 50, 1979, pp. 8034–8037.

[3]Smith, G. C., Palaniswamy, K., and Knauss, W. G., "The Application of Rate Theory to the Failure of Solid Propellants," Graduate Aeronautical Laboratories, California Institute of Technology, Report AFRPL-TR-73-54, Pasadena, CA, July 1973.

[4]Liu, C. T., "Cyclic Stress-Strain Behavior and Cumulative Damage in a Composite Solid Propellant," *Mechanical Behaviour of Materials—VI*, edited by M. Jono and T. Inoue, Pergamon, Oxford, England, UK, 1991, Vol. 3, pp. 835–840.

[5]Liu, C. T., "Crack Growth Behavior in a Composite Propellant with Strain Gradients—Part II," *Journal of Spacecraft and Rockets*, Vol. 27, No. 6, 1990, pp. 647–652.

[6]Jones, R. E., and Bradley, W. L., "Fracture Toughness Testing of Polyethylene Pipe Materials," *ASTM Special Technical Publication 995*, Vol. 1, edited by A. Saxena, J. D. Landes, and J. L. Bassani, American Society for Testing and Materials, Philadelphia, 1989, pp. 447–456.

[7]Cayard, M., "Fracture Toughness Testing of Polymeric Materials," Ph.D. Dissertation, Texas A&M Univ., College Station, TX, Sept. 1990.

[8]Williams, J. G., *Fracture Mechanics of Polymers*, 1st ed., Halsted Press, Wiley, New York, 1984.

[9]Schapery, R. A., "Correspondence Principles and a Generalized J Integral for Large Deformation and Fracture Analysis of Viscoelastic Media," *International Journal of Fracture*, Vol. 25, No. 3, 1984, pp. 195–223.

[10]Schapery, R. A., "Time Dependent Fracture: Continuum Aspects of Crack Growth," *Encyclopedia of Materials Science and Engineering*, 1st ed., Vol. 7, edited by M. B. Bever, Pergamon, Oxford, England, UK, 1986, pp. 5043–5054.

[11]Brostow, W., and Corneliussen, R. D. (eds.), *Failure of Plastics*, 1st ed., Hanser, Munich, 1986.

[12]Rice, J. R., "A Path Independent Integral and the Approximate Analysis of Strain Concentration by Notches and Cracks," *Journal of Applied Mechanics*, Vol. 35, No. 2, 1968, pp. 379–386.

[13]Anderson, T. L., *Fracture Mechanics: Fundamentals and Applications*, 1st ed., CRC Press, Boca Raton, FL, 1991, pp. 373–513.

[14]Tada, H., Paris, P. C., and Irwin, G. R., *The Stress Analysis of Cracks Handbook*, 2nd ed., Paris Publ./Del Research Corp., St. Louis, MO, 1985, pp. 2.1–2.5.

[15]Schapery, R. A., "Models for Damage Growth and Fracture in Nonlinear Viscoelastic Particulate Composites," *Proceedings of Ninth U.S. National Congress of Applied Mechanics*, edited by Y. H. Pao, American Society of Mechanical Engineers, New York, 1982, p. 237.

[16]Rice, J. R., and Rosengren, G. F., "Plane Strain Deformation Near a Crack-Tip in a Power Law Hardening Material," *Journal of the Mechanics and Physics of Solids*, Vol. 16, No. 1, 1968, pp. 1–12.

[17]Hutchinson, J. W., "Singular Behavior at the End of a Tensile Crack in a Hardening Material," *Journal of the Mechanics and Physics of Solids*, Vol. 16, No. 1, 1968, pp. 13–31.

[18]McMeeking, R. M., and Parks, D. M., "On Criteria for J-Dominance of Crack Tip Fields in Large Scale Yielding," *ASTM Special Technical Publication 668*, edited by J. D. Landes, J. A. Begley, and G. A. Clarke, American Society for Testing and Materials, Philadelphia, 1979, pp. 175–194.

[19]Shih, C. F., "Relationships Between the J-integral and the Crack Opening Displacement for Stationary and Extending Cracks," *Journal of the Mechanics and Physics of Solids*, Vol. 29, No. 4, 1981, pp. 305–329.

[20]Bucknall, C. B., *Toughened Plastics*, 1st ed., Applied Science Publishers, London, 1977, pp. 1–359.

[21]Donald, A. M., and Kramer, E. J., "Effect of Molecular Entanglements on Craze Microstructure in Glassy Polymers," *Journal of Polymer Science, Polymer Physics Edition*, Vol. 20, No. 5, 1982, pp. 899–909.

[22]Argon, A. S., "The Role of Heterogeneities in Fracture," *ASTM Special Technical Publication 1020*, edited by R. P. Wei and R. P. Gangloff, American Society for Testing and Materials, Philadelphia, 1989, pp. 127–148.

E. A. Thornton
Associate Editor